The Astrophysical Journal, 721:1656–1662, 2010 October 1 doi:10.1088/0004-637X/721/2/1656

FORMATION OF MOLECULAR HYDROGEN FROM METHANE ICE

Jiao He[1], Kun Gao[1], Gianfranco Vidali[2,4], Chris J. Bennett[2,3], and Ralf I. Kaiser[2,3]
[1] Physics Department, Syracuse University, Syracuse, NY 13244, USA
[2] Chemistry Department, University of Hawai'i at Minoa, Honolulu, HI 96822, USA
[3] NASA Astrobiology Institute, University of Hawai'i at Manoa, Honolulu, HI 96822, USA
Received 2010 April 29; accepted 2010 July 12; published 2010 September 13

ABSTRACT

To study the formation of molecular hydrogen in the wake of the processing of interstellar ices by energetic cosmic-ray particles, we investigated the interaction of energetic electrons, as formed in the track of galactic cosmic-ray particles, with deuterated methane ices (CD_4) at 11 K. The energetic electrons mimic energy-transfer processes that occur in the track of the trajectories of energetic cosmic-ray particles; deuterated methane ice was utilized to discriminate the molecular deuterium ($m/z = 4$) formed during the radiation exposure from the residual molecular hydrogen gas ($m/z = 2$) released inside the ultrahigh vacuum scattering chamber from outgassing of the stainless steel material. The ices were characterized online and in situ using Fourier transform infrared spectroscopy, while the evolution of the molecular deuterium (D_2) into the gas phase was monitored using a mass spectrometer. A mass spectrometric signal proportional to the number density of the deuterium molecules generated inside the ice and released during the irradiation was analyzed kinetically using a set of coupled rate equations. From the fit to the experimental data, we obtain activation energies for the diffusion of atomic deuterium ($E_0 = 37 \pm 1$ meV), and for the desorption of atomic ($E_1 = 32 \pm 1$ meV) and molecular deuterium ($E_2 = 32 \pm 1$ meV). These energies are placed in context and then transferred to atomic and molecular hydrogen to yield astrophysically relevant data. The experimental yield of molecular deuterium is then used to calculate the formation rate of molecular hydrogen due to cosmic-ray interaction with ice-covered grains in dense clouds.

Key words: astrochemistry – cosmic rays – infrared: ISM – ISM: molecules – methods: laboratory – molecular processes

Online-only material: color figures

1. INTRODUCTION

Molecular hydrogen is not only the most abundant molecule in space, but it also holds pivotal roles in astrophysics and astrochemistry (Combes & Pineau de Forets 2000). For instance, it helps the gravitational collapse of a molecular cloud by absorbing ultraviolet (UV) radiation and re-radiating electromagnetic energy in the infrared where the cloud is transparent, thus aiding the further contraction of the cloud. It is also a participant in ion–molecule reactions that generate a significant fraction of the 150 plus molecules that have been detected in the interstellar medium (ISM; Omont 2007). However, molecular hydrogen has no dipole moment and only a weak quadrupole moment; therefore, molecular hydrogen is detected via carbon monoxide (CO) rotational transitions which are the result of H_2–CO collisions (Habart et al. 2005). Since molecular hydrogen is destroyed by UV radiation at a known rate, the formation rate of molecular hydrogen is therefore strongly constrained. Jura (1975) obtained the rate coefficient of molecular hydrogen formation, $\mathcal{R}$ ($cm^3\ s^{-1}$). This rate must be high enough to compensate for the principal molecular hydrogen destruction mechanism, namely, UV photodissociation (Duley & Williams 1984). Since the first analysis of observations with the *Copernicus* satellite in the local diffuse cloud medium by Jura (1975), $\mathcal{R}$ has been measured in multiple ISM environments yielding values similar to the original estimate: $1 \times 10^{-17}\ cm^3\ s^{-1} < \mathcal{R} < 3 \times 10^{-17}\ cm^3\ s^{-1}$ (Gry et al. 2002; Habart et al. 2004). In dense clouds, where there is UV shielding, almost all hydrogen is in molecular form, and atomic hydrogen is mostly generated from the interaction of cosmic rays with molecular hydrogen.

In the gas phase, the formation of molecular hydrogen can occur via reactions involving electrons or ions, such as H^+ or H^- (Williams & Viti 2002). Although these reactions are a plausible route for making molecular hydrogen in the early universe, this is not so in present-time astrophysical environments; here, the degree of ionization cannot sustain those processes involving electrons or ions with rates high enough to justify observations. The radiative association of two hydrogen atoms into a stable molecule involves not only a spin-forbidden transition, but the hydrogen molecule formed is also rovibrationally excited, and this internal energy cannot be diverted via a three-body collision. Thus, it has been recognized that molecular hydrogen formation is likely to occur on surfaces of dust grains (Gould & Salpeter 1963; Hollenbach & Salpeter 1971; Hollenbach et al. 1971). The formation of molecular hydrogen in diffuse cloud environments was studied in great detail in Vidali's laboratory using polycrystalline and amorphous silicates (Pirronello et al. 1997a, 1997b; Perets et al. 2007; Vidali et al. 2007) and amorphous carbon samples (Katz et al. 1999) as analogs of bare dust grains. The formation of molecular hydrogen in dense clouds takes place on or in ices coating dust grains. These ices consist predominantly of water molecules (H_2O) arranged in the so-called high-density amorphous water solid (AWS) ice (Jenniskens & Blake 1994). Significant amounts of carbon dioxide (CO_2), CO, as well as smaller amounts of methanol (CH_3OH), formaldehyde (H_2CO), ammonia (NH_3), and methane (CH_4) are also found in ices with relative abundances that vary from cloud to cloud (Gibb et al. 2004; Ehrenfreund et al. 2007).

[4] Permanent address: Physics Department, Syracuse University, Syracuse, NY 13244, USA.

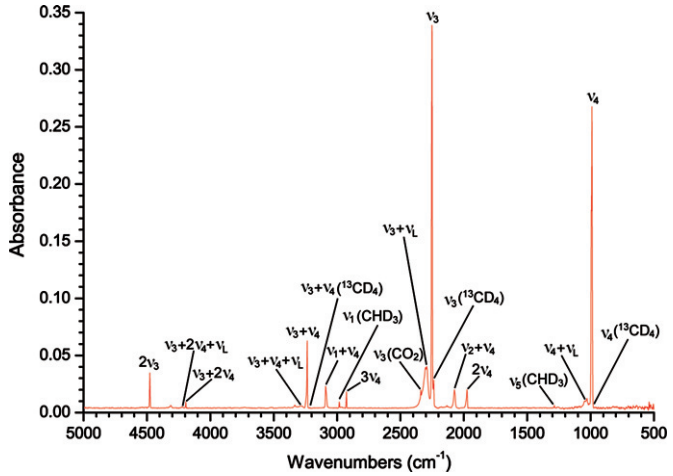

Figure 1. Infrared spectrum of deuterated methane at 11 K over the wavelength range of 5000–500 cm^{-1}. The corresponding assignments are given in Table 1. (A color version of this figure is available in the online journal.)

The formation of molecular hydrogen is readily observed when laboratory analogs of interstellar ices are subjected to irradiation of ices with protons (Brown et al. 1982; Pirronello & Averna 1988) and UV radiation (Sandford & Allamandola 1993; Watanabe et al. 2000; Watanabe & Kouchi 2008). This is of particular relevance to the interaction of simple hydrides such as methane (CH_4; Bennett et al. 2006), ammonia (NH_3; Zheng et al. 2008), and water (Zheng et al. 2006). In these ices, the energetic radiation can cause the dissociation of X–H (X = C, N, O) covalent bonds to yield hydrogen atoms which are born with excess kinetic energy of a few electron volts (eV) enabling them to diffuse through the ice. A hydrogen atom can not only migrate, but once thermalized also recombine with a second hydrogen atom to form molecular hydrogen. The excess energy can be diverted inside the ices via phonon interaction to the neighboring molecules.

In this work, we present first experimental data to systematically and quantitatively understand the formation of atomic and molecular hydrogen formed upon interaction of ionizing radiation with simple hydrides on interstellar ices. While several previous experiments have been conducted investigating the effects of UV radiation (Gerakines et al. 1996), MeV protons (Kaiser & Roessler 1998; Baratta et al. 2002; Moore & Hudson 2003), and keV electrons (Bennett et al. 2006) on methane ices, none of these studies focused on attempting to quantify the production of hydrogen. Here, we focus on the interaction of energetic electrons formed in the track of galactic cosmic-ray particles (Bennett et al. 2009) with D_4–methane ice (CD_4) to produce deuterated molecular hydrogen (D_2). An *Infrared Space Observatory* (*ISO*) survey toward young stellar objects and field stars detected methane via the ν_4 deformation mode at 7.676 μm (1303 cm^{-1}). The band position and profile were found to be consistent with the methane molecule being within a polar matrix such as water. Methane is present in interstellar dense clouds with a 1%–4% concentration with respect to water, but higher abundances (13% and 17% for Mon R2 IRS 3 and GCS 4, respectively) have been reported. We recognize that D_4–methane, in contrast to methane, is not present at an appreciable level within interstellar ices. However, the advantage of exposing D_4–methane instead of methane to energetic electrons is the formation of molecular deuterium (D_2; mass-to-charge ratio, $m/z = 4$) as opposed to molecular hydrogen (H_2); even at ultrahigh vacuum (UHV) pressures in the order of a few 10^{-11} torr, molecular hydrogen presents the most important residual gas in an experimental setup as it outgasses from the stainless steal walls of the vessel. When pure methane (CH_4) ices were irradiated, this induced a significant background level which hindered the quantification of molecular hydrogen formed during the radiation processing. This background problem can be eliminated by monitoring the formation of molecular deuterium at $m/z = 4$ during the irradiation. Here, galactic cosmic rays originating from supernova explosions have kinetic energies up to GeV; for instance, 1 MeV particles have fluxes of $\phi = 10$ particles cm^{-2} s^{-1} (Strazzulla & Johnson 1991). The cosmic rays also induce an internal UV radiation field ($\lambda < 13.6$ eV) with a fluence of $\phi = 10^3$ photons cm^{-2} s^{-1} (Prasad & Tarafdar 1983). The effects of this high-energy radiation exposure over the lifetime of an interstellar cloud of a few 10^8 yr is expected to produce significant chemical alterations of the ices condensed on the grain nuclei (Kaiser 2002).

2. EXPERIMENT

The experiment was done in the same apparatus that was used for irradiation of methane by 5 keV electrons (Bennett et al. 2006); the key experimental details are summarized here. The apparatus consists of a UHV chamber pumped to a base pressure of typically 5×10^{-11} torr by oil-free magnetically suspended turbomolecular pumps. A closed-cycle helium refrigerator is used to cool a highly polished silver (1 1 1) wafer to 11.0 ± 0.3 K; the sample is held at the center of the chamber and is freely rotatable. The deuterated methane (CD_4) ice was prepared by depositing methane (99% D, Specialty Gas Group) through a glass capillary array held 5 mm from the silver target for 5 minutes at a background pressure in the main chamber of 10^{-7} torr. A Nicolet 6700 Fourier transform infrared spectrometer (242 scans over 5 minutes from 6000 to 400 cm^{-1}, resolution 2 cm^{-1}) running in absorption–reflection–absorption mode (reflection angle 75°) is used to monitor the chemical evolution of the condensed sample online and in situ. A quadrupole mass spectrometer (Balzer QMG420) operating in residual gas analyzer mode with the electron impact ionization energy at 100 eV allows us to detect any species in the gas phase during the experiment. The deuterated methane ices were irradiated isothermally at 11.0 ± 0.3 K with 5 keV electrons generated with an electron gun (Specs EQ 22-35) at beam currents of 200 nA for 1 hr over an area of 3.2 ± 0.3 cm^2. Bearing in mind an extraction efficiency of 78.8%, this translates to 3.5×10^{15} electrons for the total exposure of 10^{12} electrons s^{-1}. After the irradiation is complete, the sample is then left isothermally for an hour before being heated to 300 K at a rate of 0.5 K $minute^{-1}$. Again, it is important to stress that deuterated methane was used so the products of the reaction caused by the irradiation could be followed against the spurious contributions of the background. This is particularly important for the detection of D_2 with a mass spectrometer, since the detection at mass 2 amu is dominated by molecular hydrogen, the background in a well-baked UHV chamber.

Figure 1 shows a typical infrared spectrum of the D_4–methane ice prior to the irradiation at 11 K; the assignments of these bands are presented in Table 1. The morphology of our deuterated methane ice deposited is expected to be primarily amorphous due to the low deposition temperatures; deposition above or annealing our sample to 22 K beforehand would result in the formation of the phase III crystalline structure which is a tetragonally oriented phase. For comparison, we have also listed the infrared band assignments from Calvani et al. (1989)

Table 1.
Infrared Absorptions of the Deuterated Methane Frost and Assignments of the Observed Bands

Position	Phase III at 17.5 K[a]	Assignment
4478	4477, 4479	$2\nu_3$
4312	...	...
4225	4222	$\nu_3 + 2\nu_4 + \nu_L$
4194	4195, 4218	$\nu_3 + 2\nu_4$
3333	...	...
3286	3277, 3287	$\nu_3 + \nu_4 + \nu_L$
3237	3225	$\nu_3 + \nu_4$
3214	3215	$\nu_3 + \nu_4$ ($^{13}CD_4$)
3084, 3090	3085, 3091	$\nu_1 + \nu_4$
2982	2993[b]	ν_1 (CHD_3)
2926	2926	$3\nu_4$
2339	...	ν_3 (CO_2)
2302, 2292	...	$\nu_3 + \nu_L$
2252	2242, 2250, 2252, 2253, 2256	ν_3
2237	2238	ν_3 ($^{13}CD_4$)
2073	2074, 2092	$\nu_2 + \nu_4$
1975, 1980	1975, 1976, 1980	$2\nu_4$
1287	1291[b]	ν_5 (CHD_3)
1029, 1037	...	$\nu_4 + \nu_L$
994, 989	985, 987, 989, 991, 992, 994, 995, 996	ν_4
981	982	ν_4 ($^{13}CD_4$)

Notes. For comparison, the band positions for deuterated methane in phase III held at 17.5 K are also given.
[a] Calvani et al. (1989).
[b] Gas phase value taken from NIST database.

reported for phase III of deuterated methane held at 17.5 K. Note the additional fine structure reported for the more ordered phase, not present in our sample confirming its amorphous character. The column density of deuterated methane (molecules cm^{-2}) can be calculated via a modified Lambert–Beers relationship (Bennett et al. 2004). From the bands $3\nu_4$, $2\nu_4$, $\nu_1 + \nu_4$, and $\nu_3 + \nu_4$ and using A values taken from Kaiser & Roessler (1998), we derive a column density of $2.9 \pm 0.5 \times 10^{17}$ molecules cm^{-2}. Taking a density of 0.67 g cm^{-3} (Kaiser et al. 1997), we can derive a thickness of 146 ± 27 nm. The electron trajectories were simulated using the CASINO code (Drouin et al. 2001). The results indicate that the distribution maximum for the energy of electrons after they have been transmitted through the sample is 4.63 ± 0.01 keV, which means that they transfer a total of 370 ± 10 eV into the sample. This value corresponds to an average linear energy transfer (LET) of 3.2 ± 0.1 keV m^{-1}, therefore exposing the sample to an average dose of 1.3 ± 0.2 eV per molecule on average.

3. RESULTS AND DATA ANALYSIS

During the irradiation, we observed a signal at $m/z = 4$, which is indicative of singly ionized molecular deuterium (D_2). No CD_4 or C_2D_6 were released during the irradiation at 11 K. In Figure 2, we show an average of four different experiments of traces of molecular deuterium gas detected by the quadrupole mass spectrometer. At time $t = 0$, the irradiation is turned on and is switched off at 3600 s. First, we discuss potential formation routes of molecular deuterium based on previous methane experiments in our group (Bennett et al. 2006), where the following reactions were identified (Bennett et al. 2006):

$$CD_4 \xrightarrow{k_1} CD_3 + D \quad (1)$$

$$(CD_4)_2 \xrightarrow{k_2} C_2D_6 + 2D \quad (2)$$

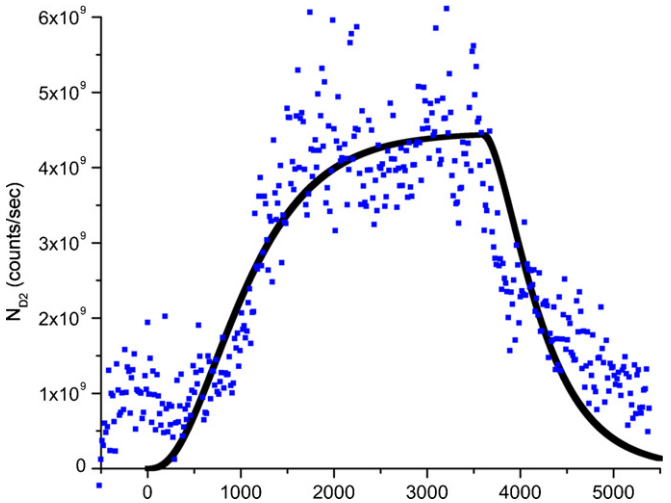

Figure 2. Number of deuterium molecules vs. time detected in the gas phase. The irradiation of the deuterated methane ice with the electrons begins at $t = 0$ and ends at $t = 3600$ s. The solid line is the result of the fit of the two distinct solutions (one for $t < 3600$ s and the other for $t > 3600$ s) of the rate equations to experimental data. The procedure of the mass spectrometer calibration is described in Zheng et al. (2006, 2008).
(A color version of this figure is available in the online journal.)

$$(CD_4)_2 \xrightarrow{k_3} C_2D_6 + D_2 \quad (3)$$

$$D + D \xrightarrow{k_4} D_2 \quad (4)$$

$$D \xrightarrow{k_5} D_{gas} \quad (5)$$

$$D_2 \xrightarrow{k_6} D_{2gas}. \quad (6)$$

The second equation symbolizes that two neighboring D_4–methane molecules (a dimer) generate deuterated ethane (C_2D_6) and two deuterium atoms or molecular deuterium (Equations (2) and (3)). The last two steps are desorption of atomic and molecular deuterium into the gas phase. k_1 through k_6 are defined as the rate constants for the reactions above.

The destruction of D_4–methane to produce atomic deuterium atoms was monitored quantitatively using infrared spectroscopy. If we assume that the only destruction pathways for CD_4 are through Equations (1)–(3), we find that $1.6 \pm 0.1 \times 10^{13}$ molecules cm^{-2} s^{-1} are destroyed by $3.1 \pm 0.3 \times 10^{11}$ electrons cm^{-2} s^{-1}; this translates in the production of around 50 ± 5 deuterium atoms per electron. The D_6–ethane (C_2D_6) that is formed in reactions (2) and (3) can be further processed into D_4–ethylene (C_2D_4), then D_2–acetylene (C_2D_2) as described in Bennett et al. (2006). Here, we find that $6.9 \pm 1.1 \times 10^{11}$ and $1.2 \pm 0.1 \times 10^{11}$ molecules cm^{-2} s^{-1} of C_2D_4 and C_2D_2 are formed, respectively. Here, the corresponding A-values (absolute intensities) for these molecules were taken from Kaiser & Roessler (1998). The additional processing of D_6–ethane and D_4–ethylene is found to contribute up to an additional 6 ± 1 deuterium atoms per electron, giving us a total average of 56 ± 6 deuterium atoms produced per electron.

In order to obtain information on the kinetics of molecular deuterium formation, we incorporate Equations (1)–(6) into two rate Equations (7) and (8), respectively, with the boundary conditions $N_D(0) = 0$, $N_{D_2}(0) = 0$, i.e., no atomic and molecular deuterium at the beginning of the irradiation:

$$\frac{dN_D}{dt} = F_D - W_D N_D - 2k_D (N_D)^2, \quad (7)$$

$$\frac{dN_{D_2}}{dt} = k_D(N_D)^2 - W_{D_2}N_{D_2}. \quad (8)$$

Here, $N_D(t)$ and $N_{D_2}(t)$ are the numbers of D atoms and D_2 molecules at time t, respectively. $W_D = \nu e^{(-E_1/kT)}$ and $W_{D_2} = \nu e^{(-E_2/kT)}$ are the desorption rates for atomic and molecular deuterium, respectively. k_D is the diffusion rate. E_1 and E_2 are the activation energies for desorption atomic and molecular deuterium, respectively. These equations were successfully used to model experiments on the formation of molecular hydrogen on surfaces of interstellar dust analogs (Katz et al. 1999), including amorphous water ice (Perets et al. 2005). In those experiments, atomic hydrogen and/or deuterium atoms were deposited on a surface of a dust grain analog and the formation of HD and/or molecular deuterium was detected in thermal programmed desorption (TPD) experiments (Vidali et al. 2005). In TPD experiments, Amiaud et al. (2006) found molecular deuterium desorption from water ice peaks at 12–26 K, depending on coverage. Watanabe et al. (2000) measured TPD peaks around 20 K for desorption of molecular deuterium deposited molecularly or produced by UV radiation of deuterated water–ice followed by the recombination of deuterium atoms. In that study, no molecular deuterium was detected as released below 20 K. The molecular deuterium released at 20 K was attributed to surface processes, while the fraction trapped in the ice was released at higher temperature. In keV irradiation of water ice, Zheng et al. 2006 found that, at comparable irradiation currents, no H_2 signal above background was detected during irradiation. In this study (see Figure 2), molecular deuterium is clearly released while the methane ice is kept at 11 K. A signal at $m/z = 4$ is also detected by the mass spectrometer during the warm-up after the irradiation; this could be due to molecular deuterium formed during the irradiation and trapped in the ice until the warm-up; alternatively, it could be due to molecular deuterium that is formed and released when deuterium atoms trapped in the ice are set in motion by the warm-up and recombine.

The first equation says that the rate of change of the number of deuterium atoms, $\frac{dN_D(t)}{dt}$, is due to the balance between the source term, F, and the losses due to desorption of deuterium atoms with rate $W_D N_D$, and due to molecular deuterium formation with rate $2k_D N_D^2$. The second equation says that the rate of change of the number of molecules formed $\left(\frac{dN_{D_2}(t)}{dt}\right)$ is due to the balance of the formation rate $(k_D N_D^2)$ and the loss rate due to evaporation, $W_{D_2}N_{D_2}$. This is conceivable, whether because one assumes that the site of molecule formation is the surface, including the surfaces of pores in the ice, or that the gain of the condensation energy propels them through the ice until they reach the surface. This conjecture is compatible with the experimental results, where the evolution of molecular deuterium from the ice occurs concomitant with the irradiation and without any thermal activation. Due to the level of noise and the impossibility of measuring $N_D(t)$ (since in the mass spectrometer the N_D signal is swamped by the signal of N_{H_2}, the main background gas), it is not feasible to determine uniquely all the parameters above. Then we proceed by making the following reasonable assumptions.

In the first equation, in first approximation, the term $2k_D(N_D)^2$ can be ignored because of the following. Consider the second equation, $\frac{dN_{D_2}}{dt} = k_D(N_D)^2 - W_{D_2}N_{D_2}$, when $\frac{dN_{D_2}}{dt} = 0$, $N_{D_2}(t) = \max$, and $k_D((N_D)|_{\max})^2 = W_{D_2}(N_{D_2})|_{\max}$. Calibration of the mass spectrometer signal using pure molecular deuterium gas enabled us to determine a sensitivity toward this species at $m/z = 4$ of $\sim 0.3 \times 10^{-2}$ A torr^{-1}, allowing us to determine a value for $(N_D)|_{\max} \sim 4.5 \times 10^9$ molecules. Therefore, $(N_{D_2})^2 = \frac{4.5\times10^9}{k_D} W_{D_2}$. Keeping in mind that at this point we want to get an order-of-magnitude estimate of N_D, we take values of E_2 and ν from the results of analysis of data of HD desorption form water ice (Perets et al. 2005), $\nu \sim 10^{12}$ s^{-1} and $E_2 \sim 50$ meV. At $T = 11$ K, $W_{D_2} \sim 10^{-3}$. Substituting in the first equation, $\frac{dN_D}{dt} = F_D - W_D N_D - 2k_D \frac{10^9}{k_D} W_{D_2} = F_D - W_D N_D - 9\times10^9 W_{D_2}$. W_{D_2} is of the same order as W_D because typically E_1 and E_2 are close (Perets et al. 2005). $N_D \sim 10^{16}$ (see equation below), and thus the last term is clearly less than the first two: $W_D N_D$; $10^{13} \gg 9 \times 10^9 W_{D_2} = 9 \times 10^9 \times 10^{-3}$. These assumptions have been verified by solving the equations and obtaining W_D, W_{D_2}, and $(N_D)|_{\max}$.

Solving the first differential equation with $2k_D(N_D)^2 \sim 0$ and for $t < 3600$ s, we get

$$N_D(t) = \frac{10^{13}}{W_D}(1 - e^{-W_D t}). \quad (9)$$

We then substitute it in the second equation and solve it; we obtain

$$N_{D_2}(t) = \frac{\left(\left(4.5\times10^9 \times e^{-W_{D_2}\times t}(2(-1+e^{W_{D_2}\times t})W_D^2 - e^{t(-2W_D+W_{D_2})}(1-4e^{W_D\times t}+3e^{2W_D\times t})W_D W_{D_2} + \right.\right.}{(2W_D^2 - 3W_D W_{D_2} + W_{D_2}^2)}$$
$$\left.\left. + \frac{e^{t(-2W_D+W_{D_2})}(-1+e^{W_D\times t})^2 W_{D_2}^2\right)\right)}{\left(2W_D^2 - 3W_D W_{D_2} + W_{D_2}^2\right)}. \quad (10)$$

At time $t = 3600$ s, the electron beam is turned off, and $N_{D_2}(t)$ starts to drop (see Figure 2). We then set $F = 0$. In Figure 2, we show solutions of the equations above using the following values of $W_D = 2.2 \times 10^{-3}$ s^{-1} and $W_{D_2} = 2.2 \times 10^{-3}$ s^{-1}. The discontinuity in the derivative of the fit is due to the fact that a different equation, with $F = 0$, is used for $t > 3600$ s. The physically interesting quantities are k_D, E_1, and E_2. From the fits, we get $E_1 = 32 \pm 1$ meV, $E_2 = 32 \pm 1$ meV, and the errors represent an estimate of the uncertainty of the ice temperature and of the range over which there is a reasonable fit (Table 2). k_D is obtained from the fit. A discussion on how to interpret these data is given further below.

Generally speaking, considering that the interaction of atoms and molecules with the surface is due to weak dispersion forces, we expect that the desorption energy for molecular deuterium

Table 2.
Activation Energies for Diffusion of Atomic Deuterium (E_0) and for the Desorption of Atomic (E_1) and Molecular Deuterium (E_2), Respectively, from Different Surfaces

Sample	E_0	E_1	E_2
CD_4[a]	37 ± 1	32 ± 1	32 ± 1
H_2O[b]	41	45	41, 53, 65, 72
H_2O[c]			30–70

Note. Energies are given in meV.
[a] This work.
[b] Top line: results obtained from rate equations using data of deuterium interacting with amorphous water ice. The model has multiple activation energies for molecular deuterium; for details, see Perets et al. 2005. Bottom line: as above, but for low-density amorphous water ice.
[c] Amiaud et al. (2006) obtained a continuous distribution of desorption energies of molecular deuterium from data of molecular deuterium adsorption on and desorption from amorphous solid water.

(E_2) is larger than for atomic deuterium (E_1), since most of the difference should be due to the different polarizability of atomic and molecular deuterium, D and D_2, respectively (Vidali et al. 1991). For example, the ratio of the binding energies of molecular and atomic hydrogen, E_2/E_1, on graphite is about 1.3 (Vidali et al. 1991). However, in our case if we try to increase E_2 by a couple of meV to come closer to the 4/3 ratio, the simulated molecular deuterium trace peaks at much later times ($t = 4000$ s) and reaches only half of the observed value. On the other hand, decreasing E_1 by a couple of meV gives yields of molecular deuterium 2 orders of magnitude lower since the deuterium atom leaves the surface quickly. This points to the fact that the just-formed molecular deuterium still possesses internal energy gained in bond formation (most likely vibrational energy). The degree of excitation of molecules formed on the surface depends critically on the nature of the surface. In this apparatus, we do not have the capability to measure the translational energy or the excitation energy of the just-formed molecules. However, we can draw inferences based on experiments done on similar ices. It has been shown in experiments of HD formation on amorphous water ice (Roser et al. 2003; Hornekær et al. 2003) that the just-formed molecules leave the surface at nearly thermal energies. In that case, the new molecules, formed in the pores of the ice, lose energy as they find their way out. But in the formation of HD on the surface of graphite, Islam et al. (2007) found that the molecules leave the surface with considerable excitation energy (vibrational quantum number $\nu = 3$ and 4).

The analysis above returns a rate of molecular deuterium formation. Since this is a mean-field result, it does not depend on the details of the mechanism(s) of diffusion. We will look at two possible scenarios: tunneling and thermally activated diffusion from thermalized, ex-suprathermal deuterium atoms. The deuterium atoms are created with suprathermal energy, but we neither know their energy distribution nor have the data on how quickly this energy is dissipated. Experiments in which the diffusion of suprathermal hydrogen atoms is invoked, such as in the hot-atom mechanism, where hydrogen atoms landing on the surface gain kinetic energy parallel to the surface from the binding energy (Harris & Kasemo 1981), are of limited help. Here, these experiments were conducted on single crystal metal surfaces (Kammler et al. 2000). Molecular dynamics calculations of hydrogen atoms landing on a water ice surface indicate that the average distance traveled is of the order of 10–60 Å (Buch & Zhang 1991; Takahashi & Uehara 2001; Al-Halabi & van Dishoeck 2007) before they were thermalized and came to rest. The simulations also find that the higher the kinetic energy of deuterium atoms, the longer the distance traveled. In the case of diffusion via tunneling, the parameter k_D would depend very sensibly on the height and width of the barrier (Cazaux & Tielens 2004). On a disordered, heterogeneous surface, tunneling is unlikely to play the dominant role (Katz et al. 1999), and thermally activated diffusion should be included as a possible mechanism. In the analysis of experiments of molecular hydrogen formation on silicate polycrystalline surface by impingement of hydrogen atoms from a thermal energy beam, it was remarked that thermally assisted tunneling can explain the experimental result in specific conditions, such as higher hydrogen coverage (Pirronello et al. 1997b). Something similar could be occurring here if the suprathermal energy of deuterium atoms is not dissipated quickly.

In the case where diffusion is by thermal activation, we can obtain the activation energy E_0 as follows. The probability that a deuterium atom reacts with another one situated at a next site within a distance r is $\frac{4}{3}\pi r^3 \frac{1}{V} \nu e^{-E_1/k_B T}$, where the probability for two atoms to be at adjacent reaction sites is $\frac{4}{3}\pi r^3 \frac{1}{V}$ and the probability for a deuterium atom to hop is $\nu e^{-E_1/k_B T}$. We take as the average distance between sites $r \sim 6$ Å, which is a typical distance between molecules in either deuterated methane or water ice. The total volume of the ice is calculated to be 4.7×10^{-5} cm^3, based on the determination of the thickness (140 nm) obtained in turn from the determination of the column density using four infrared features (see Section 2). Since $k_D = \frac{W_{D_2}(N_{D_2})|_{max}}{(N_D)|^2_{max}} = 2.2 \times 10^{-22}$ s^{-1}, $E_0 = 37.0 \pm 1.0$ meV, which is a reasonable value. A value much smaller than the desorption energies would have caused a quick molecular deuterium formation and desorption. If we had a very large value of E_0, no molecular deuterium would have formed.

Therefore, the data derived from the fits are in the range of what has been obtained in previous experiments on amorphous silicates or on/within amorphous ices using different experimental methods (Watanabe et al. 2000; Perets et al. 2005, 2007; Amiaud et al. 2007; Vidali et al. 2009), although here the mechanisms are different. The interactions are in the physical adsorption regime, where the desorption energy of atomic deuterium from crystal surfaces is in the 10–50 meV range (Vidali et al. 1991; Bruch et al. 1997). The value of the desorption energy of molecular deuterium from deuterated methane ice is smaller than the one found from water ice (30–72 meV depending on the type of ice; Perets et al. 2005; Amiaud et al. 2006; see also discussion above), but it explains the desorption of molecular deuterium at 11 K versus 20 K or higher as seen on water ice (Watanabe et al. 2000). Furthermore, given the small value of E_2, it is tempting to suppose that it is due to the sublimation of surface-created molecular deuterium.

4. ASTROPHYSICAL IMPLICATIONS

Methane is an important constituent of interstellar and planetary ices. Yeghikyan et al. (2001) found that large concentrations of methane can accumulate in collapsing clouds. Furthermore, the interaction of energetic particles or radiation with methane leads to rich chemistry, from the formation of simple hydrocarbons to polycyclic aromatic hydrocarbons (PAHs; Kaiser & Roessler 1998; Bennett et al. 2006). In dense clouds, most atomic hydrogen has been converted to molecular hydrogen. In this environment, hydrogen atoms are generated mostly by cosmic rays interacting with ices coating dust grains. Because methane is an important constituent of interstellar and cometary ices, it is important to find out what chemistry stems from hydrogen atoms interacting with radicals in methane ice. Bennett et al. (2006) studied the formation of CH_x ($x = 1$–4) and C_2H_x ($x = 1$–6) species by irradiating methane ice with keV electrons. In this work, we investigated the formation of deuterium atoms in methane ice in order to find out how efficiently deuterium atoms form deuterium molecules and to obtain physical parameters that modelers can use in their codes of the chemical evolution of molecular clouds. While we await for the results of these simulations, we can make a quick determination of the efficiency of H_2 formation in molecular clouds due to cosmic rays interacting with solid methane, and then we can compare this result to the efficiency of H_2 formation via the interaction of H atoms on the surface of ice. We proceed as follows: we assume a molecular cloud with density $n_H = 10^4$ cm^{-3}, grains with a size distribution $n(a) = c\, a^{-q}$, $q = 3.5$ (Mathis et al. 1977) with

grain size "a" from 0.03 μm to 0.3 μm (Le Petit et al. 2009) and an average density of 2.5 g cm^{-3}; we get that the number density of grains n_g is $\sim 8 \times 10^{-12}$ n_H, where n_H is the total number of protons, n(H)+2N(H_2). The formation rate is $R_{H2} = Y(H_2)\, \phi\, n_g\, A$, where $Y(H_2)$ is the yield per ion, ϕ is the cosmic-ray flux (taken to be 10 particles cm^{-2} s^{-1}), and $A \sim 3 \times 10^{-10}$ cm^{-2} is the grain cross section. Using the data from the experiment, we get $R(H_2) \sim 7 \times 10^{-19}$ cm^{-3} s^{-1} (this $R(H_2)$ should not be confused with $\mathcal{R}$ (cm^3 s^{-1}), the rate coefficient introduced earlier). A better calculation would have to follow the one done, for example, by Pirronello & Averna (1988), but the order of magnitude we get here is correct. This result can be compared with the formation rate by the association of H atoms on the surface. We have: $R(H_2) = \alpha(H_2)\, n(H)\, n_H$, where $\alpha(H_2) \sim 5 \times 10^{-17}\, (T_{gas}/300)^{1/2}$ is the effective rate coefficient (in cm^3 s^{-1}; Le Petit et al. 2009). Assuming that $\alpha(H_2)$ is essentially the same in a dense cloud (Duley & Wiliams 1984), in a dense cloud with $n_H \sim 10^4$ cm^{-3}, $T = 11$ K, and $n(H) \sim 1\%$ of $n(H_2)$, we get $R(H_2) \sim 10^{-12}$ cm^{-3} s^{-1}. This is much higher than the cosmic rate, but, as shown by Perets et al. (2005) based on actual experiments of hydrogen recombination on water ice, this efficiency is high only in a narrow range of grain temperature, while the cosmic-ray one is independent of the temperature of the grain. Thus, it is possible that cosmic-ray generation of H_2 takes over when surface-generated recombination becomes negligible. The overall impact on the H_2 budget of the cloud can be answered only by running a chemical evolution code that contains parameters deduced from experiments on surface hydrogen recombination (Perets et al. 2005) and on cosmic-ray-generated H_2 (this work).

We obtained activation energy barriers for diffusion and desorption of deuterium atoms, and for the desorption of molecular deuterium following the irradiation of deuterated methane ice with keV electrons. Differently from other laboratory studies of molecule formation in/on water ices, we find that some of the molecular deuterium sublimes *during* the irradiation at 11 K without the aid of a thermal energy input.

In our experiments, deuterium atoms are generated with energies exceeding the thermal energy of the ice (suprathermal atoms). They are likely to be more effective in finding other deuterium atoms to form molecules than thermal deuterium atoms, as they travel longer distances (Al-Halabi & van Dishoeck 2007). The molecules that are formed in the pores near the surface are more likely to move into the gas phase; they would then leave the surface without accommodating with it and using part of the energy gained from the formation of the molecule. Zheng et al. (2007) found a similar result in the interaction of keV electrons with crystalline water ice. In that case, molecular hydrogen was formed and released during the irradiation process. Additional molecular hydrogen was released during the warm-up phase. However, differently from that experiment, here additional molecular deuterium is released at around 40 K versus 100–140 K of molecular hydrogen from crystalline ice. This difference is probably due to the different types of ice (deuterated methane versus water) and hence distinct diffusion coefficients (lower ones in water ice). As the release of molecular hydrogen reported by Zheng et al. (2007) coincides with the glass to crystalline transition in water ice, it was shown that the irradiation of electrons has transformed partially or wholly a crystalline ice into an amorphous ice. Such transition is not present at 40 K in deuterated methane. However, we cannot discount the possibility that the release of hydrogen/deuterium during the warm-up in the two different ices is due to different mechanisms of formation and ejection from the surface.

Obviously, what is necessary are energy values for molecular deuterium so that modelers can utilize our data in astrophysical models. To guide us in estimating the magnitude of the isotope effect, we can look at the difference in binding energies between the two isotopes on the surface of graphite. They differ by about 7% (Vidali et al. 1991). We expect a similar difference in this case as well, since the nature of adsorption is similar (weak physical adsorption; Vidali et al. 1991). Therefore, the values of the parameters obtained from the experiments can then be used in models of the chemical evolution of dense clouds, and the relative weight given to the production of molecular hydrogen via cosmic rays versus competing processes (recombination from gas phase hydrogen atoms or hydrogen atoms generation via UV radiation), can be assessed.

G.V. acknowledges partial support from the NASA Astrobiology Institute of the University of Hawai'i and from the NSF Grant AST-0507405. The experiments in Hawaii (C.J.B. and R.I.K.) were financed by the National Aeronautics Space Administration (NASA Astrobiology Institute under Cooperative Agreement No. NNA09DA77A issued through the Office of Space Science).

REFERENCES

Al-Halabi, A., & van Dishoeck, E. 2007, MNRAS, 382, 1648
Amiaud, L., Dulieu, F., Fillion, J.-H., Momeni, A., & Lemaire, J.-L. 2007, J. Chem. Phys., 127, 144709
Amiaud, L., Fillion, J. H., Baouche, S., Dulieu, F., Momeni, A., & Lemaire, J. L. 2006, J. Chem. Phys., 124, 094702
Baratta, G. A., Leto, G., & Palumbo, M. E. 2002, A&A, 384, 343
Bennett, C. J., Jamieson, C. S., & Kaiser, R. I. 2009, ApJS, 182, 1
Bennett, C. J., Jamieson, C. S., Mebel, A. M., & Kaiser, R. I. 2004, Phys. Chem. Chem. Phys., 6, 735
Bennett, C. J., Jamieson, C. S., Osamura, Y., & Kaiser, R. I. 2006, ApJ, 653, 792
Brown, L., et al. 1982, Nucl. Instrum. Methods, 198, 1
Bruch, L. W., Cole, M. W., & Zaremba, E. 1997, Physical Adsorption: Forces and Phenomena (Oxford: Clarendon)
Buch, V., & Zhang, Q. 1991, ApJ, 379, 647
Calvani, P., Lupi, S., & Maselli, P. 1989, J. Chem. Phys., 91, 6737
Cazaux, S., & Tielens, A. G. G. M. 2004, ApJ, 604, 222
Combes, F., & Pineau des Forts, G. (ed.) 2000, in Molecular Hydrogen in Space (Cambridge: Cambridge Univ. Press)
Drouin, D., Couture, A. R., Gauvin, R., Hovington, P., Horny, P., & Demers, H. 2001, Monte Carlo Simulation of Electron Trajectory in Solids (CASINO ver. 2.42; Sherbrooke: Univ. Sherbrooke)
Duley, W. W., & Williams, W. A. 1984, Interstellar Chemistry (New York: Academic)
Dulieu, F., Amiaud, L., Baouche, S., Momemi, A., Fillion, J.-H., & Lemaire, J. L. 2005, Chem. Phys. Lett., 404, 187
Ehrenfreund, P., Charnley, S., & Botta, O. 2007, in Astrophysics of Life, ed. M. Livio, N. Reid, & W. B. Sparks (Cambridge: Cambridge Univ. Press), 1
Gerakines, P. A., Schutte, W. A., & Ehrenfreund, P. 1996, A&A, 312, 289
Gibb, E. L., Whittet, D. C. B., Boogert, A. C. A., & Tielens, A. G. G. M. 2004, ApJS, 151, 35
Gould, R. J., & Salpeter, E. E. 1963, ApJ, 138, 393
Gry, C., Boulanger, F., Nehmé, C., Pineau des Forêts, G., Habart, E., & Falgarone, E. 2002, A&A, 391, 675
Habart, E., Walmsley, M., Verstraete, L., Cazaux, S., Maiolino, R., Cox, P., Boulanger, F., & Pineau des Forêts, G. 2005, Space Sci. Rev., 119, 71
Habart, E., et al. 2004, A&A, 414, 531
Harris, J., & Kasemo, B. 1981, Surf. Sci., 105, L281
Hollenbach, D., & Salpeter, E. E. 1971, ApJ, 163, 155

Hollenbach, D., Werner, M. W., & Salpeter, E. E. 1971, ApJ, 163, 165
Hornekær, L., Baurichter, A., Petrunin, V. V., Field, D., & Luntz, A. C. 2003, Science, 302, 1943
Islam, F., Latimer, E. R., & Price, S. D. 2007, J. Chem. Phys., 127, 064701
Jenniskens, P., & Blake, D. F. 1994, Science, 265, 753
Jura, M. 1975, ApJ, 197, 575
Kaiser, R. I. 2002, Chem. Rev., 102, 1309
Kaiser, R. I., Eich, G., Gabrysch, A., & Roessler, K. 1997, ApJ, 484, 487
Kaiser, R. I., & Roessler, K. 1998, ApJ, 503, 959
Kammler, Th., Kolovos-Vellianitis, D., & Kuppers, J. 2000, Surf. Sci., 460, 91
Katz, N., Furman, I., Biham, O., Pirronello, V., & Vidali, G. 1999, ApJ, 522, 305
Le Petit, F., Barzel, B., Biham, O., Roueff, E., & Le Bourlot, J. 2009, A&A, 505, 1153
Mathis, J. S., Rumpl, W., & Nordsieck, K. H. 1977, ApJ, 217, 425
Moore, M. H., & Hudson, R. L. 2003, Icarus, 161, 486
Omont, A. 2007, Rep. Prog. Phys., 70, 1099
Perets, H. B., Biham, O., Manico', G., Pirronello, V., Roser, J., Swords, S., & Vidali, G. 2005, ApJ, 627, 850
Perets, H., et al. 2007, ApJ, 661, L163
Pirronello, V., & Averna, D. 1988, A&A, 196, 201
Pirronello, V., Biham, O., Liu, C., & Vidali, G. 1997a, ApJ, 483, L131
Pirronello, V., Liu, C., Shen, L., & Vidali, G. 1997b, ApJ, 475, L69
Prasad, S. S., & Tarafdar, S. P. 1983, ApJ, 267, 603
Roser, J. E., Swords, S., Vidali, G., Manic, G., & Pirronello, V. 2003, ApJ, 596, L55
Sandford, S. A., & Allamandola, L. J. 1993, ApJ, 409, L65
Strazzulla, G., & Johnson, R. E. 1991, in Comets in the Post-Halley Era, Vol. 1, ed. R. L. Newburn, Jr., M. Neugebauer, & J. Rahe (Astrophysics and Space Science Library, Vol. 167; Dordrecht: Kluwer), 243
Takahashi, J., & Uehara, H. 2001, ApJ, 561, 843
Vidali, G., Ihm, G., Kim, H.-Y., & Cole, M. W. 1991, Surf. Sci. Rep., 12, 133
Vidali, G., Li, L., Roser, J. E., & Badman, R. 2009, Adv. Space Res., 43, 1291
Vidali, G., Roser, J. E., Manico', G., Pirronello, V., Perets, H. B., & Biham, O. 2005, J. Phys.: Conf. Ser., 6, 36
Vidali, G., et al. 2007, J. Phys. Chem. A, 111, 12611
Watanabe, N., Horii, T., & Kouchi, A. 2000, ApJ, 541, 772
Watanabe, N., & Kouchi, A. 2008, Prog. Surf. Sci., 83, 439
Williams, D. A., & Viti, S. 2002, Annu. Rep. Prog. Chem. C: Phys. Chem., 98, 87
Yeghikyan, A., et al. 2001, MNRAS, 326, 313
Zheng, W., Jewitt, D., & Kaiser, R. I. 2006, ApJ, 639, 534
Zheng, W., Jewitt, D., & Kaiser, R. I. 2007, Chem. Phys. Lett., 435, 289
Zheng, W., Jewitt, D., Osamura, Y., & Kaiser, R. I. 2008, ApJ, 674, 1242